

Isolating long-wavelength fluctuation from structural relaxation in two-dimensional glass: cage-relative displacement

Hayato Shiba¹, Peter Keim² and Takeshi Kawasaki³

¹ Institute for Materials Research, Tohoku University, Sendai 980-8577, Japan

² Department of Physics, University of Konstanz, D-78457 Konstanz, Germany

³ Department of Physics, Nagoya University, Nagoya 464-8602, Japan

E-mail: shiba@imr.tohoku.ac.jp

Received 19 October 2017, revised 11 January 2018

Accepted for publication 18 January 2018

Published 12 February 2018



CrossMark

Abstract

It has recently been revealed that long-wavelength fluctuation exists in two-dimensional (2D) glassy systems, having the same origin as that given by the Mermin–Wagner theorem for 2D crystalline solids. In this paper, we discuss how to characterise quantitatively the long-wavelength fluctuation in a molecular dynamics simulation of a lightly supercooled liquid. We employ the cage-relative mean-square displacement (MSD), defined on relative displacement to its cage, to quantitatively separate the long-wavelength fluctuation from the original MSD. For increasing system size the amplitude of acoustic long wavelength fluctuations not only increases but shifts to later times causing a crossover with structural relaxation of caging particles. We further analyse the dynamic correlation length using the cage-relative quantities. It grows as the structural relaxation becomes slower with decreasing temperature, uncovering an overestimation by the four-point correlation function due to the long-wavelength fluctuation. These findings motivate the usage of cage-relative MSD as a starting point for analysis of 2D glassy dynamics.

Keywords: slow glassy relaxation, low-dimensional system, molecular dynamics simulation, colloids, dynamic correlation length

(Some figures may appear in colour only in the online journal)

1. Introduction

The number of spatial dimensions in a system affects the appearance of universality in phase transitions, with lower dimensions corresponding to a stronger influence of thermal fluctuations. Thus, perfect long-range order is prohibited in the lower critical dimension, which is known to be 2 for a spin system with continuous symmetry, such as the XY and Heisenberg spin models. Felix Bloch [1] first noted that global magnetisation cannot exist in one or two dimensions. This lower critical dimension was originally considered to be the marginal spatial dimension below which the phase transition vanishes. It was later proven to be a special universal phase

transition, which became known as the ‘Kosterlitz–Thouless transition’ [2]. In the low-temperature phase, the translational order is quasi-long-ranged, because of the long-wavelength fluctuation. This is in contrast to systems with more than four dimensions (i.e. the upper critical dimensions), for which fluctuation is associated with the mean-field universality class.

A two-dimensional (2D) crystal also possesses continuous symmetry at the thermodynamic limit of infinite system sizes N . In 1934, Peierls considered a solid with harmonic interactions and fixed connectivities [3]. We denote the displacement of a particle from the lattice position as \mathbf{u}_i . The relative thermal displacement between a pair of distant atoms $|\mathbf{u}_i - \mathbf{u}_j|$ increases as a function of the interatomic distance r_{ij} as

$$\langle |\mathbf{u}_i - \mathbf{u}_j|^2 \rangle \propto \log r_{ij}, \quad (1)$$

meaning that the thermal strain compounds logarithmically with N , finally diverging at the macroscopic limit. This argument was previously considered as evidence that 2D solids cannot exist in terms of long-range translational order.

At present, however, it is widely accepted that perfect long-ranged orientational order does exist in 2D crystals. The melting of those crystals is described by the so-called Kosterlitz–Thouless–Halperin–Nelson–Young (KTHNY) theory [4, 5], based on the dissociation of topological defects of Kosterlitz–Thouless type. In the scenario described by the KTHNY theory, emergence of finite elastic moduli is an essential feature that renders a 2D crystal distinct from other states [5–7]. Note, also, that this concept can be fruitfully transferred to 2D amorphous solids. Recent developments with regard to computational power and simulation techniques have allowed more precise characterisation of the melting transition of 2D crystals. In particular, the problem of whether the transition is continuous or weakly first order has come into focus once more and stimulated recent works, both simulation-based [8–11] and experimental [12–15].

The question as to whether the glass transition is dimensionality dependent is intriguing. Recent work has focused on the glass transition at the limit of infinite spatial dimensions [16–18]; the expectation is to observe the mean-field behaviour of the glassy dynamics above the upper critical dimension ($d = 8$) of the random first-order transition theory. It was expected that a 2D glass would behave similar to its three-dimensional (3D) counterpart [19, 20]. Recently, however, significant differences have been observed between 2D and 3D glasses in computer simulation [21]. The present authors [22, 23] and Vivek *et al* [24] have noted that those differences can be explained by considering fluctuations that obey the Mermin–Wagner theorem at long wavelengths. Such long-wavelength fluctuation is found to strongly affect the standard time correlation functions, such as the MSDs and intermediate scattering functions. It has also been shown that the long-wavelength fluctuations are independent of the structural changes by using either broken bond functions [22] or cage-relative quantities [22–24].

In this paper, we investigate the glassy fluctuation and relaxation by analysing molecular dynamics simulation results of lightly supercooled liquid in two dimensions, with particular focus on the cage-relative variable, which is key to separate the glassy structural relaxation from the long-wavelength fluctuation. The purpose of this study is to make a clear separation between the structural rearrangements and the acoustic fluctuations over the entire time range in the glassy dynamics, from the time scales of the cage vibration to α relaxations, focusing on the cage-relative displacements and their variants. Special attention is placed on the crossover from short- to long-term diffusion in the plateau region of the MSD. Note that the typical timescales of the Mermin–Wagner fluctuations and structural relaxations exhibit different dependence on N and temperature T .

The remainder of this paper is organised as follows. In section 2, relevant background information regarding fluctuations in 2D crystals and glass is provided. The methods employed

in this study are described in section 3, and the results are presented and discussed in section 4. A brief summary is given in section 5.

2. Background: fluctuations in 2D crystals and glass

2.1. Mermin–Wagner fluctuation in 2D elastic body

We first address a 2D glass at a fixed T , regarding it as an isotropic elastic solid and beginning with an assembly of atoms that are displaced by thermal fluctuations from their initial position \mathbf{R} . The instantaneous position of each particle at time t is then given by $\mathbf{r}(t) = \mathbf{R} + \mathbf{u}(\mathbf{R}, t)$. The displacement field $\mathbf{u}(\mathbf{R}, t)$ is described as a superposition of plane waves with different wave-numbers \mathbf{k} , as follows:

$$\mathbf{u}(\mathbf{R}, t) = \left(\frac{L}{2\pi}\right)^D \int \mathbf{u}_k(t) \exp(i\mathbf{k} \cdot \mathbf{R}) d^D k. \quad (2)$$

Here, D indicates the spatial dimension, which is equal to 2 in our discussion, and L denotes total length of the system.

In an elastic medium at finite T , extended acoustic modes exist in the continuum limit, and their long-wavelength contributions can be treated as a gas of independent phonons, equivalent to the Debye model for harmonic solids. The equipartition of energy among the independent modes gives $m\omega_k^2 |\mathbf{u}_k|^2 = k_B T$, where m is the average particle mass, ω_k is the frequency of each mode with wavenumber \mathbf{k} , and k_B is the Boltzmann constant. Based on this assumption, the mean-squared thermal displacement $\langle |\mathbf{u}|^2 \rangle = \left(\frac{L}{2\pi}\right)^D \int \langle |\mathbf{u}_k|^2 \rangle d^D \mathbf{k}$ can be expressed as

$$\langle |\mathbf{u}|^2 \rangle = \frac{Dk_B T}{m} \int \frac{g_D(\omega)}{\omega^2} d\omega, \quad (3)$$

where $g_D(\omega)$ denotes the vibrational density of state (vDOS) of the long-wavelength phonons obeying the linear dispersion relation $\omega_k = ck$ (c is the sound velocity). For $D = 2$, the integral in equation (3) exhibits an infrared divergence, because the vDOS is given by $g_D(\omega)/\omega = (2\pi c^2)^{-1}$ under the Debye approximation. This asymptotic Debye behaviour should appear in the very-low-frequency region beyond the well-known boson peak [25–30]. For the 2D systems, the existence of the boson peak may be difficult to detect in experiment [31–33]; however, simulation results indicate that the boson peak has a subtle but definite existence in a 2D glass [34, 35].

Recently, the vDOS was confirmed to approach $g_D(\omega)$ asymptotically for 2D disk glassy systems with soft-core 12th [22] and harmonic repulsions [35]. Further, plane-wave-like Debye behaviour was demonstrated experimentally through a trajectory analysis of a 2D colloidal glass former [33].

The divergence is logarithmic, but has a sizeable effect. The amplitude A_p of the thermal vibration can be readily estimated by introducing the minimum frequency $\omega_{\min} = 2\pi/t_c$ in the integral of equation (3), $t_c = L/c$ is the time before a sound wave traverses the entire system

$$A_p^2 \sim \frac{k_B T}{\pi} \left(\frac{1}{\mu} + \frac{1}{K + \mu} \right) \log \left(\frac{L}{\sigma} \right). \quad (4)$$

Further, σ denotes the mean particle radius providing the minimum length scale in the system and μ and K are the shear and bulk moduli, respectively. Use is made of a trivial relation $A_p^2 = 2\langle|\mathbf{u}|^2\rangle$, where it is stated that the amplitude A_p^2 is twice the MSD for all modes exhibiting Gaussian thermal fluctuations. As there are *equal* numbers of longitudinal and transverse sound modes in 2D, each with velocities c_L or c_T , respectively, we have the expression above (equation (4)) [22]. Then, $c_L = \sqrt{\mu/\rho}$ and $c_T = \sqrt{(K + \mu)/\rho}$, with the mass density $\rho = mn$ and n being the number density.

For a prevalent class of glasses, its relaxation is attributed to an accumulation of local structural rearrangements represented by intermittent jumping motions of particles to escape the cage created by their neighbours [36–39]. This local process cannot couple with longer-wavelength modes and has marginal influence on the size-dependent fluctuation. In fact, it is consistent with the observation that the size dependence is limited only to the scale of heterogeneous motion for several kinds of 3D glassy liquids [40–42]. On further observation, the long-wavelength modes are found to induce cooperative motion in 3D fragile glass formers [43, 44], but the link between the cooperativity and slow relaxation is weak and remains to be clarified. However, for 2D glasses and glassy liquids, the magnitude of the long-ranged fluctuation increases with increased N and the dynamics is directly affected up to a long time scale comparable to t_c [22]. It should be noted that the system size dependence in equation (3) is nothing but a different expression of Mermin–Wagner theorem, the root of the KTHNY transition in 2D melting. For this reason, this fluctuation can be named as ‘Mermin–Wagner fluctuation’ [23], expected ubiquitously in a 2D glass.

2.2. Realisation in colloidal experiments

Recently, molecular dynamics simulations have been conducted for a 2D supercooled liquid with large system sizes [21, 22, 45]. For a molecular dynamics simulation of particles with short-ranged interactions, simulations can be parallelised with spatial-decomposition techniques—as a result, computation load is simply proportional to the system size N . Therefore, simulation performance scales linearly with the number of nodes, which is the reason why it has recently become possible to perform molecular dynamics simulations of large-scale fluctuations in an assembly of millions of particles, over a decade of orders of time steps.

The first experimental observations of 2D glassy long-wavelength fluctuations have also been realised [23, 24], motivated by the observation of the dimensionality dependence in [21]. Such fluctuations are ubiquitously expected for a wide range of solids (crystalline or amorphous) confined in two dimensions, because the logarithmic increase in amplitude is an immediate consequence of the linear elasticity. Graphene might be regarded as an ideal candidate with 2D structure. However, the A_p term in equation (4) can be estimated to be 10^{-6} Å for a sheet with a size of meter order, if typical values for elasticity are assumed ($\sigma \sim 1$ Å, $\mu \sim 440$ GPa) [46, 47].

In fact, other mechanisms such as out-of-plane fluctuations may govern the rippling motions in graphene.

Soft matter systems, on the other hand, provide a unique experimental environment for long-wavelength fluctuation. Indeed, colloidal particles confined in a planar geometry have been considered by several groups [15, 48–55]. For experiments on 2D colloidal glasses, A_p can exceed 0.2σ , which is of sub-micrometer order for 2D binary colloidal systems. The softness of colloidal ensembles is due to the fact that the interaction energies between particles are of the same order of magnitude as the atomic system. As the particle distances are 10^4 – 10^6 times larger, the energy densities and, therefore, elastic constants, are 10^{-8} – 10^{-12} and 10^{-12} – 10^{-18} times smaller in 2D and 3D, respectively, compared to those of atomic systems. Because of this softness, long-wavelength excitations are easily activated by thermal energy in colloidal ensembles [23, 24, 33]. The easily accessible length scales at single-particle level and the easily accessible time scales of individual motion are at the expense of the accessibility of the long-term behaviour. While colloidal experiments can typically span five decades, experiments on molecular glasses usually address 10 to 20 decades, at the expense of single-particle information.

2.3. Separating structural relaxation: cage dynamics

Recent simulations [22] and experiments [23, 24] have clarified that long-wavelength Mermin–Wagner fluctuations exist in 2D glassy systems, even if they lack crystalline structure. Furthermore, the infrasound divergence of such an enhanced fluctuation is shown to be independent of the structural relaxation. Standard time correlation functions based on the density field, including MSDs, fail to characterise such structural relaxation for large 2D systems, because the local density is strongly smeared by the transient vibrations. The effect of Mermin–Wagner fluctuations significantly larger than the local scale of the discrete density is simply an affine translation. Local rearrangements such as those due to particles escaping the cages created by their nearest neighbours, and the inherent glassy relaxation, are decoupled from the Mermin–Wagner fluctuations.

In these studies [22–24], cage-relative variables, which are explained in detail below, are considered. They are defined on the basis of a displacement of a particle relative to its neighbours (defined at an initial time), relating its motion to the local coordinate frame. Through this approach, the N dependence in the MSD disappeared and decoupling of the orientational and translational relaxations reported in [21] disappear, indicating that the local rearranging motion is successfully depicted using cage-relative variables. Note that correlations calculated from global variables depend on two contributions: the local rearrangements of the glassy relaxations and the long-wavelength fluctuations. Unlike standard quantities, cage-relative quantities are not affected by long wavelength density fluctuations. Therefore, the comparison between standard and cage-relative correlation functions offers the possibility of quantitative characterisation of the

amplitudes of the Mermin–Wagner fluctuations, as actually achieved in a recent simulation [22].

Evaluating the amplitudes in this manner yields compatible results with Mermin–Wagner fluctuations evaluated ‘*a priori*’ using elastic constants at zero temperature [22]. Deviations appear for increased N , when the time-scale of the long-wavelength vibrations becomes comparable to that of the structural relaxation. Apart from cage-relative displacements, the bond-breakage function extracts rearrangements or complementary information on an atomistic level, and has also been successfully employed in simulation by two of the present authors [22]. This function characterises the change in the number of neighbour particles with respect to time, and has been employed to evaluate dynamic length scales [45, 56–58].

3. Methods

3.1. Simulation details

In this paper, the simulation data of the 2D binary 50:50 soft-core potential system examined in [22] are analysed. The pairwise interaction is given as a function of distance r by

$$v_{\alpha\beta}(r) = \epsilon \left(\frac{\sigma_{\alpha\beta}}{r} \right)^{12}, \quad (5)$$

for $r \leq r_c = 2.21\sigma_1$, i.e. within the cutoff distance r_c . The cubic smoothing function $v_{\alpha\beta}(r) = B(a - r)^3 + C$ is applied for distances $r > r_c$, with a , B , and C satisfying continuity conditions at $r = r_c$ up to the second derivative of $v_{\alpha\beta}(r)$. The indices $\{\alpha, \beta\} \in \{1, 2\}$ represent the particle species. The size and mass ratios are set to $\sigma_2/\sigma_1 = 1.4$ and $m_2/m_1 = (\sigma_2/\sigma_1)^2$, with $\sigma_{\alpha\beta} = \frac{1}{2}(\sigma_\alpha + \sigma_\beta)$, and the interaction energy ϵ is the same for all pairs.

In the remainder of this paper, the results are presented in reduced units of σ_1 , ϵ/k_B , and $t_0 = \sqrt{m_1\sigma_1/\epsilon}$ for the length, T , and time, respectively. The simulations begin from the liquid state at $T = 2.5$; then, we rapidly cool to the target T values and allow the system to relax under the Langevin thermostat over a sufficiently long lapse of time ($5 \times 10^5 t_0$ for $T = 0.64$). All the dynamic quantities and correlations in the following sections are calculated from further simulations, which are all performed based on the Newtonian dynamics and without heat baths. The temperature is set to $T = 0.64$ for almost all simulations; however, cases involving other T are presented in section 4.2.

3.2. Cage-relative displacements and their time-correlation function

After rapid cooling of the liquid, the viscosity increases significantly and the structure becomes frozen, transforming into a glass. In glassy systems, the MSD

$$M(t) = \left\langle \frac{1}{N} \sum_{i=1}^N |\Delta \mathbf{r}_i(t)|^2 \right\rangle, \quad \Delta \mathbf{r}_i(t) = \mathbf{r}_i(t) - \mathbf{r}_i(0), \quad (6)$$

exhibits two-step relaxation behaviour due to the intermittent jump motion, with N being the total particle number. Before and after the plateau regions, the MSD exhibits an increase

as a function of time t . The short-term regions are typically proportional to t^2 if the dynamics of each particle obeys the Newtonian law, and in the long term become proportional to t , indicating slow diffusion. For intermediate time scales, a plateau with height $M(t_p)$ appears, with t_p being a time corresponding to oscillatory motion inside the cage [59]. $M_p(t_p)$ is approximately equal to the squared amplitude of the thermal oscillation [60] and is an increasing function for increasing T . This height is typically a few percent of the interparticle distance for strongly supercooled fluids up to a value of the order of a tenth of the interparticle distance in the vicinity of melting, at least for small N . Those observations are compatible with Lindemann-like arguments for *small* 2D crystals. It is worth mentioning that the short-term dependence in colloidal systems is linear to t ; because of the viscous solvent, the particles obey Brownian motion with overdamped dynamics and diffusive behaviour [49].

To disentangle the effects of the jump motions and long-wavelength fluctuations, we employ the cage-relative displacement

$$\Delta \mathbf{r}_i^{\text{CR}}(t) = \Delta \mathbf{r}_i(t) - \frac{1}{N_i^{\text{n.n.}}} \sum_{j \in \text{n.n.}} \Delta \mathbf{r}_j(t) \quad (7)$$

and cage-relative MSD

$$M^{\text{CR}}(t) = \left\langle \frac{1}{N} \sum_{i=1}^N |\Delta \mathbf{r}_i^{\text{CR}}(t)|^2 \right\rangle \quad (8)$$

defined as its mean square, where the summation indicates the neighbours of particle i and $N_i^{\text{n.n.}}$ represents the number of neighbours. As obvious from the definition, the motion of the particle relative to its neighbours is quantified. Note that the concept of cage-relative displacement was originally introduced for analysis of the melting of 2D crystals, so that the effect of the Mermin–Wagner fluctuations could be eliminated efficiently [12, 61]. Recently, this concept has been applied to the analysis of 2D glassy systems [22–24, 33, 62, 63].

4. Results

4.1. Long-wavelength Mermin–Wagner fluctuation after removal of cage-relative contributions

The MSD is a quantity that is directly affected by long-wavelength fluctuation. Because the equilibrium position (note that this is no longer a lattice position for glassy liquids and amorphous solids) of particle i does not change long before the α relaxation, the MSD is given by [45]

$$M(t) = \frac{1}{N} \sum_i \langle |\mathbf{u}_i(t_0) - \mathbf{u}_i(t_0 + t)|^2 \rangle, \quad (9)$$

at the plateau time t_p , where $\mathbf{u}_i(t)$ represents the displacement of particle i from its equilibrium position. Under the assumption that the cross correlation $N^{-1} \sum_i \langle \mathbf{u}_i(t_0) \cdot \mathbf{u}_i(t_0 + t) \rangle$ decays for a fast acoustic damping, the plateau becomes

$$M(t_p) = 2 \langle |\mathbf{u}|^2 \rangle. \quad (10)$$

The authors have recently found that the MSD exhibits N dependence in its plateau region for 2D glassy systems originating from the Mermin–Wagner fluctuation [22, 23]. This behaviour is attributed to the N dependence of the mean squared fluctuation amplitude $A_p^2 = 2\langle |\mathbf{u}|^2 \rangle$ of equation (4), on the basis that only the long-wavelength Mermin–Wagner contributions are acting. However, for a quantitative comparison between the plateau height and fluctuation amplitude, it is necessary to further eliminate the in-cage motion.

The cage-relative MSD is employed to eliminate the long-wavelength fluctuation, and is found to terminate the N dependence of the MSD originating from this fluctuation [22, 23]. The cage-relative MSD reflects particle motion relative to its neighbours. In the short-term, far before α relaxation without changes in the neighbours, this quantity involves contributions from in-cage vibration; thus, it is possible to isolate the long-wavelength contribution. On this basis, in a recent paper [22], the difference between the MSD and the cage-relative MSD

$$\Delta^{\text{CR}}(t) = M(t) - M^{\text{CR}}(t), \quad (11)$$

was considered at $t = t_p$, to evaluate the A_p^2 of the long-wavelength fluctuation. This quantity can be loosely interpreted as indicating the cage-irrelevant part of the MSD.

For sufficiently low T , the plateau is well-defined over a wide time span between the β and α relaxations, allowing precise evaluation of A_p^2 . Hence, we can correctly calculate the long-wavelength vibration. However, if the relaxation time is too short for a crossover with the vibration time scale to occur, $\Delta^{\text{CR}}(t)$ is affected by local rearrangement of the neighbour particles. This means that the quantity can no longer be exploited for quantitative evaluation of the vibrations. Therefore, an applicability limit clearly applies to $M^{\text{CR}}(t)$ if α relaxation becomes too short, rendering it difficult to completely separate the acoustic fluctuation and diffusion. This problem becomes more critical for larger N , because the time period of the acoustic fluctuation is proportional to $t_c = L/c$ in a 2D system, meaning that the time scale of the plateau increases linearly with the system length.

In this section, we evaluate the N dependence of the A_p^2 of the long-wavelength fluctuation in equation (4). In the supercooled system considered here, the α relaxation time is sufficiently short that the plateau height of the MSD (and $\Delta^{\text{CR}}(t)$) is affected by the slow diffusion. In figure 1, $\Delta^{\text{CR}}(t)$ is plotted for different N . A plateau is apparent in a time region similar to that of the original MSD. However, after t_p of the original MSD, growth with time also appears. This growth is weaker than the linear diffusion in the original MSD, exhibiting the subdiffusive asymptote $\Delta^{\text{CR}}(t) \sim Ct^{0.67}$ at the long-term limit, where C is estimated for each N through fitting. The reason for the increase in $\Delta^{\text{CR}}(t)$ is that the average displacement of the neighbours in equation (7) no longer represents the motion of the cage, because these neighbours are also involved in the local particle rearrangement. This is due to the average displacement given in equation (7), which is associated with the contributions of the particles with jump motions to the configuration changes.

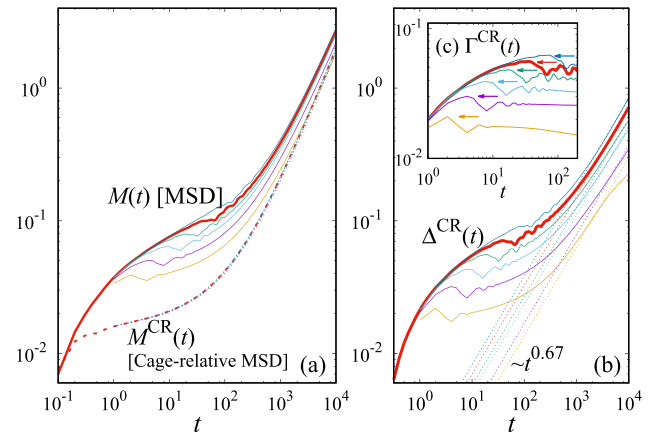


Figure 1. (a) System size N dependence of MSD $M(t)$, indicated by solid lines. (Bold solid line: dependence for $N = 64000$. Bottom to top: small to large N , for $N = 250, 1000, 4000, 16000, 64000$ (bold), and 256000, at fixed temperature $T = 0.64$.) The dotted lines indicate the cage-relative MSD $M^{\text{CR}}(t)$, where the data for different system sizes collapse into one line. (b) N dependence of ‘cage-irrelevant’ part of MSD $\Delta^{\text{CR}}(t)$, indicated by solid lines (bold solid line: $N = 64000$. Bottom to top: small to large N , as in (a), at fixed temperature $T = 0.64$.) The thin dotted lines indicate the fitting by $Ct^{0.67}$ in the ‘subdiffusive’ regions (c) MSD of cage-irrelevant vibration $\Gamma^{\text{CR}}(t)$ after subtraction of subdiffusive asymptote in $\Delta^{\text{CR}}(t)$. For all the data in the figure, the temperature is fixed ($T = 0.64$).

For the largest system size ($N = 256000$), where t_p is more retarded than for smaller systems, the height of $\Delta^{\text{CR}}(t_p)$ is still affected by the long-term behaviour. Before comparing the plateau heights of this $\Delta^{\text{CR}}(t)$ and the MSD, we attempt to eliminate the effect of long-term dynamics, by subtracting the value of the subdiffusive asymptote:

$$\Gamma^{\text{CR}}(t) = \Delta^{\text{CR}}(t) - Ct^{0.67}. \quad (12)$$

As the contribution of the local particle rearrangement is removed to leave only the effect of the long-wavelength acoustic fluctuations, the quantity $\Gamma^{\text{CR}}(t)$ represents the MSD of the cage-irrelevant fluctuation. This quantity is plotted in the inset of figure 1. Compared with the previous quantities $M(t)$ and $\Delta^{\text{CR}}(t)$, the plateau regions extend to longer times and their heights can be accurately estimated.

Figure 2 shows the heights of the plateaus of the cage-irrelevant MSD $\Delta^{\text{CR}}(t_p)$ and its fluctuation component $\Gamma^{\text{CR}}(t_p)$ after subtraction of the subdiffusive asymptote, together with the original MSD $M(t_p)$ (the same data as in [22]), with all the plateaus assumed to occur at the same time $t = t_p$. The data for $L = 561.8$ ($N = 256000$) are added for $\Delta^{\text{CR}}(t_p)$, while the MSD plateau $M(t_p)$ can be evaluated to $L = 280.9$ only (t_p is taken as being the same for the three quantities). We note that the long-wavelength contribution to A_p^2 in equation (4) is evaluated under Debye approximation with the sound velocities at temperatures very close to zero. The sound velocities change by approximately 20% for the temperature primarily considered in this paper. At higher temperatures, sound waves can be influenced by nonlinear

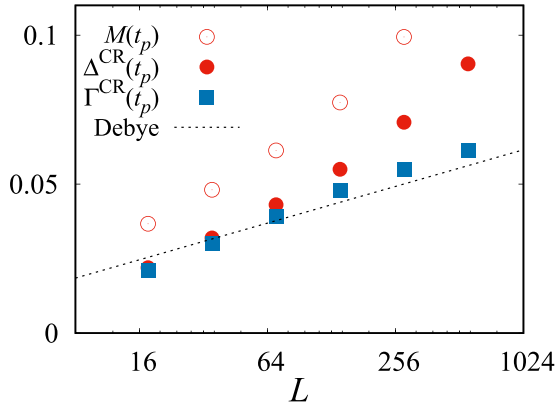


Figure 2. Plateau heights of MSD $M(t_p)$ and difference between $M(t_p)$ and cage-relative MSD $\Delta^{\text{CR}}(t_p)$ (open and filled circles, respectively) plotted as functions of linear system size L , with the particle numbers being $N = 250, 1000, 4000, 16000, 64000$, and 256000 from left to right. Except for $N = 256000$ for $\Delta^{\text{CR}}(t_p)$, the data are taken from [22]. The dotted line is the Debye asymptote for two dimensions estimated using equation (4), for sound velocities estimated at $T \simeq 0$. The corrected residue $\Gamma^{\text{CR}}(t_p)$ is also plotted (square boxes).

interactions between atoms. Further consideration is required for more precise characterisation of the acoustic waves at finite temperatures.

Here, the Mermin–Wagner-type argument should hold well for an amorphous solid simulated at a low-enough temperature; this is because the plateau heights should become free from crossovers with the diffusive region. The difficulties in evaluating the plateau heights are limited to the lightly cooled case. The N dependence of the thermal fluctuation can be clarified further through a thorough analysis of the acoustic normal modes (dynamic structure factors) over the full range of wave-vectors and frequencies; we plan to address this topic in a forthcoming study.

4.2. Dynamic correlation lengths

From the above discussions, it is plausible that the N dependence of the plateau heights is attributed to the Mermin–Wagner fluctuation, which induces an infinite correlation length, and that the dependence can be removed using a quantity that specifically characterises the intermittent particle motions involved in structural rearrangement. Thermal fluctuations between 2D and 3D glassy systems are fundamentally different.

The purpose of this section is to quantitatively characterise the glassy relaxation after elimination of the Mermin–Wagner fluctuation. For the dynamics of glasses, the dynamic correlation length is one of the well-accepted quantities that is intimately linked to slow relaxation of the system. However, the most popular four-point correlation length ξ_4 has been shown to overestimate the dynamic correlation length for large N [22, 45], because the displacement becomes larger as a result of the Mermin–Wagner fluctuation. This dynamic correlation length is evaluated by evaluating the heterogeneity in the overlap function $W_i(t) = \Theta(a - |\Delta \mathbf{r}_i(t)|)$ representing

whether particle configurations are overlapping between times separated by t , where $\Theta(x)$ is Heaviside’s step function. Characterising the dynamic correlation length in this manner, we cannot avoid to involve the particle that are moving coherently with neighbouring particles.

If the dynamic correlation length is defined instead on the basis of a quantity characterising the particle motion relative to the neighbours, this problem can be avoided. For instance, by taking the change in the nearest neighbour pair as a dynamic measure, named as broken-bond correlation function [22, 45], the associated dynamic correlation length ξ_B has been revealed to be N -independent, successfully qualified as a quantity representing to what extent the structural relaxation becomes heterogeneous, after separating the large-scale fluctuations.

In this section, we newly introduce another dynamic correlation length that is free from the effect of the large-scale fluctuation. In order to eliminate the effect of large-scale fluctuation in the four-point correlation analysis, we replace the displacement $\Delta \mathbf{r}_i(t)$ by the cage-relative displacement, and define a ‘cage-relative’ overlap function

$$D_j(t) = \Theta(a - |\Delta \mathbf{r}_j^{\text{CR}}(t)|), \quad (13)$$

with the threshold value a set to $0.3\sigma_1$, a typical value utilised for the usual overlap function. This means that, if the distance spanned by the particle’s motion *relative to its neighbours* exceeds a , $D_j(t)$ becomes zero; otherwise, it is unity. The degree of heterogeneity of the dynamics is then characterised as a dynamic susceptibility, defined in a similar manner to the standard four-point susceptibility as

$$\chi_{\text{CR}}(t) = N [\langle D(t)^2 \rangle - \langle D(t) \rangle^2], \quad D(t) = \frac{1}{N} \sum_{j=1}^N D_j(t). \quad (14)$$

It is assumed that the increase of the dynamic susceptibility reflects the degree of correlation between the relaxation processes, which also applies to the present susceptibility. The structure factor for the cage-relative overlap function is defined by

$$S_{\text{CR}}(k, t) = \frac{1}{N} \langle R(\mathbf{k}, t) R(-\mathbf{k}, t) \rangle, \quad (15)$$

$$R(\mathbf{k}, t) = \sum_{j=1}^N D_j(t) \exp[-i\mathbf{k} \cdot \mathbf{r}_j(0)]. \quad (16)$$

Then, ξ_{CR} can be estimated by fitting $S_{\text{CR}}(k, t)$ to the Ornstein–Zernike function

$$S_{\text{CR}}(k, t_{\text{CR}}) = \frac{S_{\text{CR}0}}{1 + [k\xi_{\text{CR}}]^\alpha} \quad (\alpha = 2), \quad (17)$$

at the peak time t_{CR} of $\chi_{\text{CR}}(t)$. At this time t_{CR} , the degree of heterogeneity in the structural changes is evaluated in the maximised manner.

Figure 3 shows $\chi_{\text{CR}}(t)$ for various N , with the temperature fixed at $T = 0.64$. It is obviously independent of the system size. The standard four-point dynamic susceptibility $\chi_4(t)$ for the 2D glassy liquid, which has been investigated recently

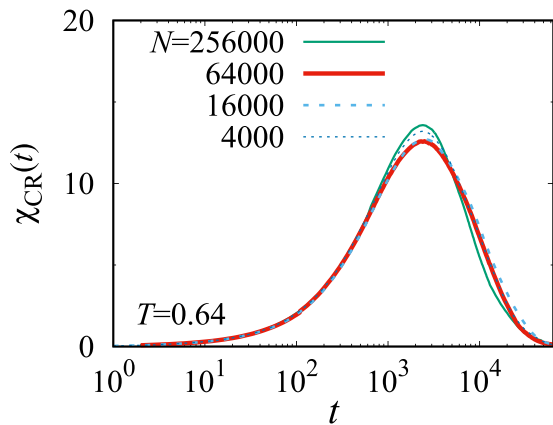


Figure 3. System size N dependence of dynamic susceptibility $\chi_{CR}(t)$ defined with cage-relative spatiotemporal correlation function, indicated by solid lines.

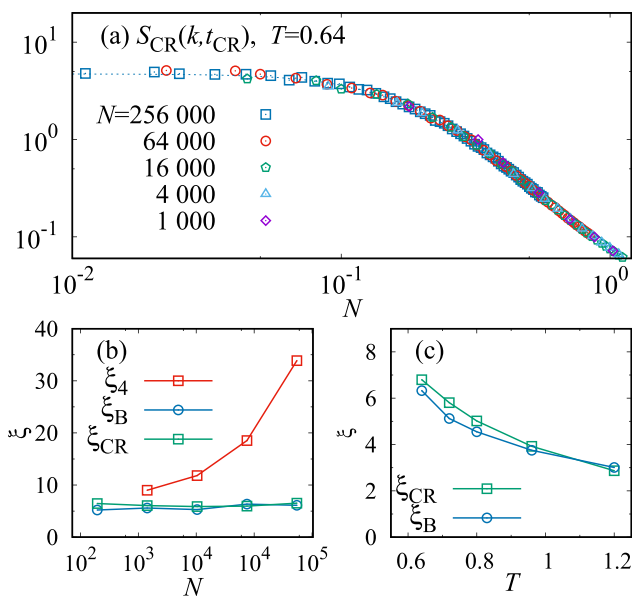


Figure 4. (a) System size N dependence of structure factor $S_{CR}(k, t_{CR})$ for cage-relative overlap function and for a fixed temperature $T = 0.64$, in two dimensions. (b) Cage-relative, broken-bond, and four-point dynamic correlation lengths ξ_{CR} , ξ_B , and ξ_4 plotted as functions of N (in terms of total particle number N), for fixed temperature $T = 0.64$. (c) Cage-relative and broken-bond dynamic correlation lengths ξ_{CR} and ξ_B plotted as functions of temperature T for fixed system size of $N = 256000$.

[22], exhibits periodic oscillation that is N dependent, in a sharp contrast to $\chi_{CR}(t)$. By changing the measure of mobility from the simple displacement to that relative to the neighbours, the dynamic susceptibility is altered to characterise the dynamic fluctuation, with the effect of long-wavelength Mermin–Wagner fluctuation omitted.

In figure 4(a), $S_{CR}(k, t_{CR})$ is plotted at a fixed temperature $T = 0.64$. The data for different N collapse into one, meaning that the spatial heterogeneity is similar for the different N . In a recent paper [22], the corresponding structure factors are also evaluated for the four-point and broken-bond correlation functions, where the former is found to be strongly N -dependent, and the latter is not.

In figure 4(b), we show the N dependence of the dynamic correlation lengths at the same temperature $T = 0.64$ for the cage-relative overlap functions ξ_{CR} , for the broken bond functions ξ_B , and for the simple overlap function (so-called four-point length) ξ_4 . Each of them is evaluated from the corresponding structure factors. In line with the result for the structure factors, we find that ξ_{CR} and ξ_B exhibit no N dependence, whereas ξ_4 shows a strong finite size effect. For the cage-relative overlap functions, the dynamic correlation ξ_{CR} is found to be similar to that of broken-bond function ξ_B .

Finally, we evaluate both ξ_{CR} and ξ_B for different T for a fixed system size $N = 256000$, as shown in figure 4(c). The dynamic correlation lengths ξ_{CR} and ξ_B are found to be similar over all T ranges. Moreover, these lengths grow as the T decreases to approach the glass transition. This result indicates that both quantities are eligible candidates for dynamic correlation lengths characterising the dynamic heterogeneity associated with the inherent relaxation motion, after isolating the long-wavelength Mermin–Wagner fluctuation.

5. Conclusion

In this study, we performed molecular dynamics simulation analysis of structural relaxation in 2D glassy dynamics. The long-wavelength fluctuation can be separated from the structural relaxation by using the cage-relative MSD, defined to characterise particle motion relative to its cage, including particle escape motion from its cage and the short-ranged motion. It was found that, if the time scale is sufficiently short that only small changes in the caging particles occur, the long-wavelength fluctuation can be well quantified. We can evaluate the amplitude of the long-wavelength Mermin–Wagner fluctuation as a ‘cage-irrelevant part’ ($\Delta^{CR}(t)$) by subtracting the cage-relative contribution. In 2D glassy systems, however, the time-scale of the long-wavelength fluctuation is incremented linearly with the system size. This time scale can be comparable to that of the glassy structural changes. If the system is excessively large or is only slightly supercooled, the cage may break, leading to an increment in the cage-relative MSD. The cage-irrelevant part deviates from the squared fluctuation amplitude predicted by the Debye asymptote. We amended the deviation by introducing a tentative quantity $\Gamma^{CR}(t)$, and retrieved the original squared amplitude of the thermal amplitude.

The values of the dynamic correlation lengths were evaluated using the cage-relative MSD, and were similar to that estimated using the bond-breakage variables; however, the four-point correlation function failed to yield a correct measurement result [22]. This result indicates that the former two variables successfully capture the heterogeneous nature of the local rearrangement associated with the slow structural changes, following elimination of the transient acoustic fluctuation. Thus, cage-relative displacement successfully characterises the dynamic heterogeneity on the α relaxation time scale, as well as the bond-breakage variables.

We conclude that the cage-relative displacement well characterises the intermittent particle motion out of the cage, associated with the inherent structural relaxation. On a time scale

before multiple jumps out of the cage take place for each particle (typically $t \lesssim t_{CR}$), the MSD is partitioned quantitatively into long-wavelength fluctuation and the structural relaxation. For a quantitative description of the longer-term dynamics, for large N and high temperature, the analysis method should be improved to capture the inherent structural changes with multiple jumps out of the cages.

It is still an open question whether the nature of 2D glass transition is affected by the long-wavelength fluctuation. The relevance of the structural relaxation to the glassy properties e.g. inherent structures, localisation of the vibration, stress relaxation mechanisms, etc can be examined for large systems. Analysis of the dynamics presented in this paper, together with the broken-bond analysis, will be helpful to resolve this issue.

Acknowledgments

H S and T K are financially supported by JSPS KAKENHI, Grants No. JP25103010 and JP16H06018, respectively. H S is also thankful for financial support from the Building Consortia for the Development of Human Resources in Science and Technology, the Ministry of Education, Culture, Sports, Science, and Technology, Japan. The numerical calculations were performed on the SGI Altix ICE XA at the Institute for Solid State Physics, University of Tokyo, Japan.

ORCID iDs

Hayato Shiba  <https://orcid.org/0000-0002-4170-3699>
Takeshi Kawasaki  <https://orcid.org/0000-0001-8036-8435>

References

- [1] Bloch F 1930 *Z. Phys.* **61** 206–19
- [2] Kosterlitz J M and Thouless D J 1973 *J. Phys. C: Solid State Phys.* **6** 1181–203
- [3] Peierls R 1934 *Helv. Phys. Acta* **7** 81–3
- [4] Halperin B I and Nelson D R 1978 *Phys. Rev. Lett.* **41** 121–4
- [5] Nelson D R and Halperin B I 1979 *Phys. Rev. B* **19** 2457–84
- [6] Sengupta S, Nielaba P and Binder K 2000 *Phys. Rev. E* **61** 6294–301
- [7] Kosterlitz J M 2016 *Rep. Prog. Phys.* **79** 026001
- [8] Shiba H, Onuki A and Araki T 2009 *Europhys. Lett.* **86** 66004
- [9] Bernard E P and Krauth W 2011 *Phys. Rev. Lett.* **107** 155704
- [10] Kapfer S C and Krauth W 2015 *Phys. Rev. Lett.* **114** 035702
- [11] Zu M, Liu J, Tong H and Xu N 2016 *Phys. Rev. Lett.* **117** 085702
- [12] Zahn K and Maret G 2000 *Phys. Rev. Lett.* **85** 3656–9
- [13] Deuschländer S, Puertas A M, Maret G and Keim P 2014 *Phys. Rev. Lett.* **113** 127801
- [14] Li B, Wang F, Zhou D, Peng Y, Ni R and Han Y 2016 *Nature* **531** 485–8
- [15] Thorneywork A L, Abbott J L, Aarts D G A L and Dullens R P A 2017 *Phys. Rev. Lett.* **118** 158001
- [16] Charbonneau P, Ikeda A, Parisi G and Zamponi F 2012 *Proc. Natl Acad. Sci.* **109** 13939–43
- [17] Kurchan J, Parisi G and Zamponi F 2012 *J. Stat. Mech.* P10012
- [18] Rainone C, Urbani P, Yoshino H and Zamponi F 2015 *Phys. Rev. Lett.* **114** 015701
- [19] Harrowell P 2006 *Nat. Phys.* **2** 157–8
- [20] Bayer M, Brader J M, Ebert F, Fuchs M, Lange E, Maret G, Schilling R, Sperl M and Wittmer J P 2007 *Phys. Rev. E* **76** 011508
- [21] Flenner E and Szamel G 2015 *Nat. Commun.* **6** 7392
- [22] Shiba H, Yamada Y, Kawasaki T and Kim K 2016 *Phys. Rev. Lett.* **117** 245701
- [23] Illing B, Fritschi S, Kaiser H, Klix C L, Maret G and Keim P 2017 *Proc. Natl Acad. Sci. USA* **114** 1856–61
- [24] Vivek S, Kelleher C P, Chaikin P M and Weeks E R 2017 *Proc. Natl Acad. Sci. USA* **114** 1850–5
- [25] Taraskin S N and Elliott S R 1997 *Phys. Rev. B* **56** 8605–22
- [26] Schirmacher W, Diezemann G and Ganter C 1998 *Phys. Rev. Lett.* **81** 136–9
- [27] Duval E, Boukenter A and Achibat T 1990 *J. Phys.: Condens. Matter* **2** 10227–34
- [28] Monaco G and Giordano V M 2009 *Proc. Natl Acad. Sci. USA* **106** 3659–63
- [29] Xu N, Wyart M, Liu A J and Nagel S R 2007 *Phys. Rev. Lett.* **98** 175502
- [30] Monaco G and Mossa S 2009 *Proc. Natl Acad. Sci. USA* **106** 16907–12
- [31] Ghosh A, Chikkadi V K, Schall P, Kurchan J and Bonn D 2010 *Phys. Rev. Lett.* **104** 248305
- [32] Chen K et al 2010 *Phys. Rev. Lett.* **105** 025501
- [33] Klix C L, Maret G and Keim P 2015 *Phys. Rev. X* **5** 041033
- [34] Shintani H and Tanaka H 2008 *Nat. Mater.* **7** 870–7
- [35] Mizuno H, Shiba H and Ikeda A 2017 *Proc. Natl Acad. Sci. USA* **114** E9767–74
- [36] Schober H R, Oligschleger C and Laird B B 1993 *J. Non-Cryst. Solids* **156–8** 965–8
- [37] Weeks E R and Weitz D A 2002 *Phys. Rev. Lett.* **89** 095704
- [38] Chaudhuri P, Berthier L and Kob W 2007 *Phys. Rev. Lett.* **99** 060604
- [39] Ciamarra M P, Pastore R and Coniglio A 2016 *Soft Matter* **12** 358–66
- [40] Kim K and Yamamoto R 2000 *Phys. Rev. E* **61** R41–4
- [41] Berthier L, Biroli G, Coslovich D, Kob W and Toninelli C 2012 *Phys. Rev. E* **86** 031502
- [42] Karmakar S and Procaccia I 2012 *Phys. Rev. E* **86** 061502
- [43] Karmakar S, Dasgupta C and Sastry S 2016 *Phys. Rev. Lett.* **116** 085701
- [44] Peng H L, Schober H R and Voigtmann T 2016 *Phys. Rev. E* **94** 060601(R)
- [45] Shiba H, Kawasaki T and Onuki A 2012 *Phys. Rev. E* **86** 041504
Shiba H, Kawasaki T and Onuki A 2017 *Phys. Rev. E* **95** 069901 (erratum)
- [46] Abraham F F 1981 *Phys. Rep.* **80** 340–74
- [47] Thompson-Flagg R C, Moura M J B and Marder M 2009 *Europhys. Lett.* **85** 46002
- [48] Pieranski P 1980 *Phys. Rev. Lett.* **45** 569–72
- [49] König H, Hund R, Zahn K and Maret G 2005 *Eur. Phys. J. E* **18** 287–93
- [50] Yunker P, Zhang Z, Aptowicz K B and Yodh A G 2009 *Phys. Rev. Lett.* **103** 115701
- [51] Zheng Z, Wang F and Han Y 2011 *Phys. Rev. Lett.* **107** 065702
- [52] Keim P, Maret G, Herz U and Von Grünberg H H 2004 *Phys. Rev. Lett.* **92** 215504
- [53] Gasser U 2009 *J. Phys.: Condens. Matter* **21** 203101
- [54] Zahn K, Lenke R and Maret G 1999 *Phys. Rev. Lett.* **82** 2721–4
- [55] Peng Y, Wang Z, Alsayed A M, Yodh A G and Han Y 2010 *Phys. Rev. Lett.* **104** 205703
- [56] Yamamoto R and Onuki A 1997 *J. Phys. Soc. Japan* **66** 2545–8

- [57] Yamamoto R and Onuki A 1998 *Phys. Rev. E* **58** 3515–29
- [58] Kawasaki T and Onuki A 2013 *Phys. Rev. E* **87** 012312
- [59] Binder K and Kob W 2005 *Glassy Materials and Disordered Solids* (Singapore: World Scientific)
- [60] Kob W and Andersen H C 1995 *Phys. Rev. E* **51** 4626–41
- [61] Zheng X H and Earnshaw J C 1998 *Europhys. Lett.* **41** 635–40
- [62] Mazoyer S, Ebert F, Maret G and Keim P 2009 *Europhys. Lett.* **88** 66004
- [63] Hu Y C, Tanaka H and Wang W H 2017 *Phys. Rev. E* **96** 022613